Plasma Physics Aspects of Tunnel-Ionized Gases

W. P. Leemans, C. E. Clayton, W. B. Mori, K. A. Marsh, A. Dyson, and C. Joshi
Electrical Engineering Department, University of California, Los Angeles, California 90024
(Received 25 July 1991)

Tunnel-ionized plasmas have been studied through experiments and particle simulations. Experimentally, x-ray measurements show that the plasma temperature is higher for a circularly polarized laser-produced plasma compared to when linear polarization is used. A higher parallel temperature than expected from the single-particle tunneling model was observed through Compton scattering fluctuation spectra. Simulations indicate that stochastic heating and the Weibel instability play an important role in plasma heating in all directions and isotropization.

PACS numbers: 52.40.Nk, 52.50.Jm

The ionization of atoms by strong electromagnetic fields can in the high-intensity and/or long-wavelength limit be modeled as a process in which an electron tunnels through the Coulomb barrier suppressed by the electric field [1]. This model is valid when $\gamma=(E_{\rm ion}/2\Phi_p)^{1/2}\ll 1$, where $E_{\rm ion}$ is the ionization potential of the charge state under consideration and Φ_p is the ponderomotive potential of the laser. Although tunneling ionization of single atoms has been studied with both 10- and 1-μm laser pulses [2,3], no detailed study of macroscopic plasmas produced using this mechanism has been made. These plasmas may be unique because the laser intensity profile $I(\mathbf{r},t)$ and polarization could be used to determine the initial parallel and perpendicular temperatures $(T_\parallel, T_\perp)$ of the electrons, density n, and ionization state Z. Such plasmas have applications in the areas of recombination x-ray lasers [4] and various collective accelerator schemes [5]. Moreover, the possibility of tailoring the initial 3D distribution functions may allow the study of basic kinetic and parametric instability theory issues in plasma physics. In this Letter we explore the plasma physics aspects of gases ionized via tunneling ionization through experiments and supporting particle-in-cell computer simulations. Our experimental work shows that in the "plasma regime" $T_\parallel$ is higher than expected from the single-particle tunneling model and that ionization-induced refraction clamps the density to $n<10^{-3}n_c$. Here n_c is the critical density. Simulations indicate that stochastic heating [6] and the Weibel [7] instability play a crucial role in plasma heating and isotropization.

In the experiment, a CO_2 laser beam (up to 100 J contained in an approximately triangular pulse having a 150-ps rise time and a 350-ps fall time) was focused to a spot size $2w_0$ of 340 μm into a vacuum chamber containing up to 5 Torr of Ar or H_2 gas, using an $f/9$ parabolic mirror. The peak laser intensity in vacuum was around 3×10^{14} W/cm^2. At this intensity, an estimate based on Gauss' law shows that, for fill pressures P exceeding 1 mTorr, the space-charge potential is large enough to confine most of the electrons against the ponderomotive potential of the laser. The space-charge-dominated plasma was produced over approximately two Rayleigh lengths, $2z_0$, and was diagnosed by (a) viewing the forward laser harmonic emission, (b) collective Thomson scattering of a 0.5-μm beam to probe $2\mathbf{k}_0$ density fluctuations, and (c) by measuring the x-ray emission from the plasma. Using the tunneling-ionization rate equation [8] and neglecting any pump depletion, we find that in Ar gas full ionization (to $Z=1$) is attained for our experimental parameters in approximately 25 ps once the threshold of 6×10^{13} W/cm^2 is exceeded [9]. If the laser intensity rises beyond 10^{14} W/cm^2, further ionization to $Z=2$ can occur [3].

In these experiments the laser wavelength is 10 μm and $\gamma\ll1$; ionization occurs via the tunneling process rather than via multiphoton ionization. We believe that the evidence for plasma formation by tunneling comes from odd-harmonic emission from the plasma. When linear polarization is used the ionization proceeds in stepwise fashion at twice the laser frequency generating a nonlinear current $J(l\omega_0,lk_0)=-evn$, $l=3,5,7,\ldots$, which acts as a source term for odd-harmonic emission [8]. The frequency spectrum of the transmitted or forward-scattered laser light was found to contain discrete lines $(\Delta\lambda/\lambda<10^{-3})$ at the second, third, and fifth harmonic of the laser frequency. As expected from the tunneling mechanism, the third and the fifth harmonic were found to decrease in magnitude as the degree of ellipticity α of the laser polarization was increased. The measured ratio [10] P_3/P_1 is in reasonable agreement with the expected theoretical value [8]. Other mechanisms such as relativistic effects [11], the nonlinear susceptibility $\chi^{(3)}$ of the media [12], and ionization due to correlated collisions for generating the odd harmonics are relatively unimportant [10]. The second-harmonic emission observed in the experiment was found to be nearly independent of polarization and cannot be explained by any of the above mechanisms. Simulations to be discussed later show that the second-harmonic emission originates from the edges of the plasma, where the density gradients are the steepest, suggesting that the source for the even harmonics is the nonlinear current $\mathbf{J}_2=-en\mathbf{v}_2=-(e^2/4m\omega)n\nabla E^2$ [13].

In the absence of plasma effects, the evolution of the electron energy distribution can be calculated assuming classical interaction of the newly born electrons with the ionizing electromagnetic fields [2]. 1D calculations show

that upon reaching full ionization an anisotropic quasi-Maxwellian distribution with $T_\perp \approx 150$ eV and $T_\parallel \ll 1$ eV is produced for linearly polarized light. For circularly polarized light, a ring distribution with a major radius (transverse to the incident laser beam wave vector $\mathbf{k}_0$) of 2.5 keV and a minor radius of 1 keV with $T_\parallel$ of only 4 eV is generated. Therefore, one might expect that fully ionized plasmas with controllable $T_\perp$ and negligible $T_\parallel$ can be produced by tunneling ionization. This possibility has been experimentally investigated.

Our main density and $T_\parallel$ diagnostic is based on the detection of electron-density fluctuations with $k_p = 2k_0$ excited by the laser beam through either stimulated Raman (SRS) [14] or Compton (SCS) [15] scattering. If the tunnel plasmas have very low values of $T_\parallel$ as the single-particle model suggests, then $k_p\lambda_D \ll 1$ and SRS should have a very large growth rate, whereas for large $T_\parallel$ and $k_p\lambda_D$ on the order of 1, SCS may occur. Here λ_D is the Debye length. The scattered light from $2k_0$ density fluctuations was wavelength (0.2 Å resolution) and time resolved (10 ps resolution) with a spectrograph-streak-camera combination. However, it is not possible to follow the time evolution of the ionization process using this technique since the ionization rate is comparable to the homogeneous, time-independent growth rate for the Raman-Compton instability [10,16]. Thus the instabilities are suppressed until the ionization process is saturated by depletion of the neutrals or ionization-induced refraction.

Experiments show that the high-frequency density fluctuations have a broad frequency spectrum consistent with Compton rather than Raman scattering. The evolution of one such spectrum from a plasma produced in a static fill of 1.1 Torr of H_2 is depicted in Fig. 1(a). At early times [Fig. 1(b)], the spectrum can be fitted quite well applying the usual Compton theory [15] to give $n \approx 6\times10^{15}$ cm^{-3} and $T_\parallel \approx 75$ eV. This temperature is already much higher and the density much lower than that predicted by the single-particle model. At later times the spectrum develops structure and broadens to both higher and lower frequencies. About 140 ps after the onset of SCS, the spectrum resembles incoherent Thomson scattering from a thermal plasma rather than from a collective mode. These are still driven fluctuations (albeit in the strongly driven regime) as evidenced from the absence of scattered light on the blue side. The most probable cause of the frequency broadening of the spectrum is a continued increase of $T_\parallel$ of the plasma. As will be seen later, this is believed to be due to the Weibel instability, which is an electromagnetic plasma instability driven by an anisotropic electron distribution. Even at higher fill pressures, the SCS spectra indicated very low peak densities with $n \leq 10^{-3} n_c$. To independently bracket the range of plasma density, resonant optical mixing was carried out using various combinations of lines of the CO_2 laser [10]. A resonant plasma response was observed at fill pressures

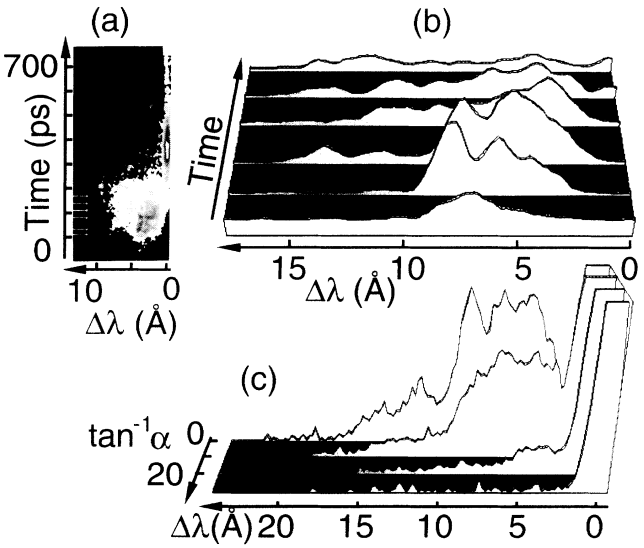

FIG. 1. (a) Streak-camera image of the Thomson-scattered probe beam in a H_2 plasma ($P = 1.1$ Torr). Although not shown here, there was no blueshifted spectral feature visible in the original data. The white bar at the top indicates the location of a 100× attenuator for SBS. The peak intensity is 1.5×10^{14} W/cm^2. (b) Line outs of streak data taken along the direction of the arrows in (a). (c) Time-integrated streak-camera images of the Thomson-scattered probe beam in H_2 plasmas ($P = 1$ Torr) for different degrees of ellipticity α of the laser polarization ($\tan^{-1}\alpha = 45$ for circular polarization).

corresponding to a plasma density around 8×10^{15} cm^{-3} but not 1.2×10^{17} cm^{-3} [17]. Also, at the higher pressures a significant amount of the laser energy was found to be refracted out of the original cone angle of the laser beam. This is shown in Fig. 2(a). The onset of refraction in H_2 is more gradual than in Ar because the lighter H^+ ions can radially move during the laser pulse and thereby relax the radial density gradients. These gradients are initialized by the ionization process since the ionization rate has a strong nonlinear dependence on the laser field. This onset of refraction over a narrow range of pressures is taken as evidence for density clamping due to ionization-induced refraction. The effect of this refraction is to prevent the laser intensity from being significantly above the ionization threshold for a sufficient duration to fully ionize the gas [17]. At these low densities, collisional processes should be relatively unimportant on the time scales of the laser pulse.

We explored the possibility of laser plasma instability control by varying the polarization of the laser beam. The main effect of changing the laser polarization is to drastically alter the initial transverse distribution of electron energies. If these distributions isotropize rapidly, then $k_p\lambda_D$, and therefore the damping rate for high-frequency electron fluctuations, can be varied. As we increased α the fluctuations due to stimulated Brillouin scattering (SBS) were unaffected whereas the high-

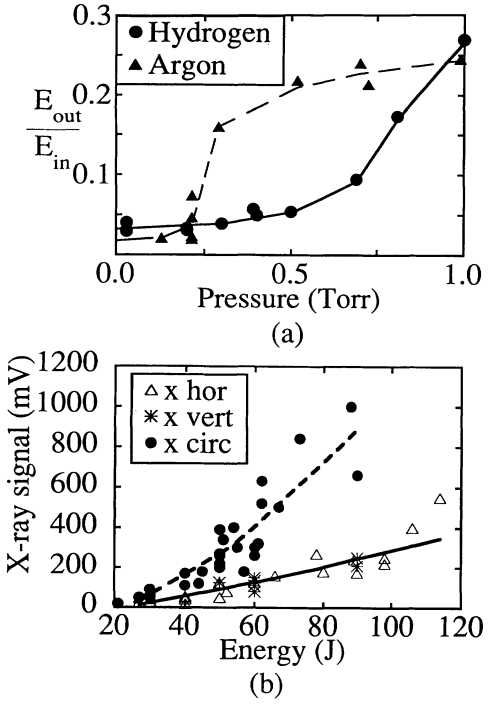

FIG. 2. (a) Ratio of the laser energy refracted outside of the original cone angle of the beam to the incident laser energy as a function of neutral gas fill pressure. The energies are measured by two cross-calibrated detectors. The saturation of the refracted energy at 30% of the incident energy is due to the limited solid angle viewed by the calorimeter measuring the refracted beam energy. (b) The x-ray emission from argon plasmas (fill pressure of 280 mTorr), as a function of laser energy for different polarizations.

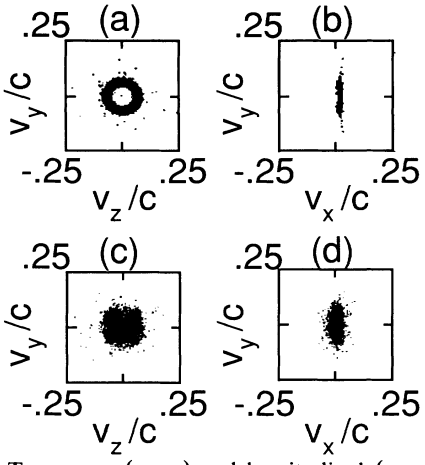

FIG. 3. Transverse (v_y,v_z) and longitudinal (v_y,v_x) velocity space without [(a) and (b)] and with "plasma" effects [(c) and (d)]. In (a) and (b) the simulation was done on a 1D grid. The maximum density was $n/n_c = 10^{-8}$. The laser rise and fall time was $500\omega_0^{-1}$. The major (minor) radius of the ring corresponds to a "temperature" of 1 keV (20 eV). In (c) and (d) the simulation was done on a 2D grid ($200c/\omega_0 \times 125c/\omega_0$). The peak density was $4\times10^{-4}n_c$. The laser beam was collimated and had a Gaussian transverse profile with a beam diameter of $30c/\omega_0$. The peak field strength corresponded to $0.1v_{osc}/c$ for both the 1D and 2D simulations. The transverse (longitudinal) temperature at $T = 1200\omega_0^{-1}$ is ≈ 500 eV (50 eV).

frequency fluctuations became weaker and were eventually completely suppressed for $\alpha \geq 0.6$ [Fig. 1(c)]. These observations are consistent with an increase in $T_\parallel$ in going from linear to circularly polarized light. However, the inferred values for $T_\parallel$ are still anomalously higher than the single-particle predictions.

To obtain an independent estimate of the plasma temperature and to explore the possibility of plasma temperature control through polarization of the ionizing laser light, soft-x-ray emission above 800 eV was measured using a calibrated silicon surface-barrier detector with Be and Mylar filters. Figure 2(b) shows three sets of data: linear polarization with the detector looking (i) along and (ii) transverse to the electric field, and (iii) circular polarization. A significant difference in x-ray flux was seen between linear and circular polarization, as expected from the tunnel-ionization model. However, no significant difference was seen between looking transverse and along the electric field for the linear polarization. The increase of x-ray flux with laser energy can simply be attributed to the increase of plasma volume at higher laser intensity. A temperature estimate was obtained by measuring the relative x-ray yield through two different filter combinations for a constant density (fill pressure) plasma and the same laser energy [18]. Assuming that the x rays are emitted through bremsstrahlung from an isotropized Maxwellian distribution, we estimate a plasma temperature of 450 ± 150 eV (180 ± 50 eV) for circular (linear) polarization. These temperatures are within a factor of 2 of what might be expected from a laser beam which has its intensity clamped close to the ionization threshold due to refraction.

To understand the origin of the initial $T_\parallel$ and its further increase with time, simulations were carried out using the 2D fully relativistic, electromagnetic particle-in-cell code WAVE which includes collisional and tunneling ionization [19]. Simulations were designed to isolate the roles of parametric instabilities, space-charge effects and refraction, and the Weibel instability. In all cases a circularly polarized beam was launched from the left-hand boundary with a peak $v_{osc}/c = 0.1$, where v_{osc} is the oscillatory velocity of the electron in the laser field. The laser propagates in the x direction. Time is normalized to ω_0^{-1} and space to c/ω_0. When a new electron and ion are created they are injected with an isotropic velocity of $10^{-5}c$. For extremely low densities, $n/n_c = 10^{-8}$, the electron distribution functions obtained were in excellent agreement with those expected from the single-particle model [Figs. 3(a) and 3(b)].

Simulations with a fully ionized density of $10^{-2}n_c$ and a laser rise time of $750\omega_0^{-1}$ were done to isolate the

high-frequency instabilities (SRS and SCS). In 1D, SRS was seen to grow to large levels ($\delta n/n = 0.3$) because of a very low initial $T_\parallel$ ($k_p\lambda_D \ll 1$), and saturate due to particle trapping. In 2D, however, where the beam was focused into the middle of the simulation box, SRS was suppressed because $T_\parallel$ at the end of the ionization was already large. Instead SCS occurred at a reduced level, consistent with experimental observations. A possible explanation for this high $T_\parallel$ at that time is that the electrons are born at positions where electric fields, for small f-number focusing and/or strong refraction, have a substantial longitudinal component. This in turn results in a significant longitudinal drift velocity component (i.e., $T_\parallel$) of the electrons. In addition, the electrons, retained by the ion space charge, continue to interact with both the applied electromagnetic fields and the space-charge fields. Their phase-averaged guiding-center energy can increase in a stochastic fashion [6] leading to hotter plasmas. In a 2D simulation with $n/n_c = 4\times10^{-4}$, too low for the parametric instabilities or refraction to occur, it was indeed found that at the end of the laser pulse, the plasma had a higher than expected $T_\parallel$ (50 eV vs 2 eV in the 1D computations) [Figs. 3(c) and 3(d)]. When the density was increased to $n/n_c = 0.1$, strong refraction of the beam was observed with the beam waist moving towards the laser leading to further stochastic heating. The simulations are in agreement with a theoretical model [10] which gives a maximum refraction limited density on axis produced by a Gaussian beam in a static gas of $n/n_c < (4\lambda/\pi z_0) \times (\ln\alpha/2\alpha)^{1/2}$ for $\alpha < 7.4$ and an effective pulse length longer than z_0. Here λ is the wavelength and α the ratio of peak intensity to ionization threshold intensity. For our parameters this leads to $n < 10^{-3}n_c$. This value is consistent with the maximum density inferred from the SCS spectra and optical mixing. Furthermore, the onset of refraction at around 0.2 Torr for Ar also indicates a similar value for the density. We therefore believe that ionization-induced refraction explains the observed density clamping.

The isotropization of the electron distribution functions due to the Weibel instability was isolated by running a 1D simulation with $n/n_c = 5\times10^{-3}$ and a short laser pulse ($1000\omega_0^{-1}$) to suppress parametric instabilities. The measured growth rate of the long scale length magnetic-field characteristic of the Weibel instability was in reasonable agreement with the theoretical prediction of $\gamma \approx 2\times10^{-3}\omega_0$ [10,20]. The saturation value of the electron cyclotron frequency ω_{ce} of the magnetic-field mode with the maximum growth rate [20] was found to be $0.005\omega_0$. However, temperature isotropization occurred over a slower time scale, $\tau \approx 2\pi/\omega_{ce}$. Using the theoretical growth rate for our experimental parameters we find that the Weibel instability will completely isotropize the electrons in roughly 75 ps (180 ps) for circular (linear) polarization. This is consistent with the observed broadening of the SCS spectrum [Fig. 1(b)] as discussed earlier. Although the simulations discussed here were carried out with a circularly polarized beam, similar effects occur with a linearly polarized beam.

In conclusion, the properties of tunnel-ionized plasmas have been studied through experiments and particle simulations. Odd-harmonic emission characteristic of stepwise tunnel ionization and density clamping due to ionization-induced refraction are observed. Experimentally, x-ray measurements show that the plasma temperature is higher for a circularly polarized laser-produced plasma compared to when linear polarization is used. Furthermore, longitudinal temperatures are higher than those expected from a single-particle model as evidenced from SCS spectra. Simulations indicate that stochastic heating and the Weibel instability play an important role in plasma heating and isotropization.

We thank J. M. Wallace of LANL for providing us with WAVE. This work was supported by the U.S. Department of Energy Contract No. DE-AS03-83-ER40120, and the LLNL University Research Program.

[1] L. V. Keldysh, Zh. Eksp. Teor. Fiz. **47**, 1945 (1964) [Sov. Phys. JETP **20**, 1307 (1965)].
[2] P. B. Corkum *et al.*, Phys. Rev. Lett. **62**, 1259 (1989); F. Yergeau *et al.*, J. Phys. B **20**, 723 (1987).
[3] S. Augst *et al.*, Phys. Rev. Lett. **63**, 2212 (1989).
[4] N. H. Burnett and P. B. Corkum, J. Opt. Soc. Am. B **6**, 1195 (1989).
[5] "Plasma Based High-Energy Accelerators," edited by T. Katsouleas [IEEE Trans. Plasma Sci. **15**, 192 (1987)].
[6] D. W. Forslund *et al.*, Phys. Rev. Lett. **54**, 558 (1985); J. N. Bardsley *et al.*, Phys. Rev. A **40**, 3823 (1989).
[7] E. S. Weibel, Phys. Rev. Lett. **2**, 83 (1959).
[8] F. Brunel, J. Opt. Soc. Am. **7**, 521 (1990).
[9] Experimentally, no significant plasma formation was detected for an average laser intensity less than 6×10^{13} W/cm^2.
[10] W. P. Leemans, Ph.D. dissertation, UCLA, 1991 (unpublished).
[11] P. Sprangle *et al.*, Phys. Rev. A **41**, 4463 (1990).
[12] J. F. Ward and G. H. C. New, Phys. Rev. **185**, 57 (1969).
[13] J. Meyer and Y. Zhu, Phys. Fluids **30**, 890 (1987).
[14] C. J. Walsh *et al.*, Phys. Rev. Lett. **53**, 1445 (1984).
[15] W. P. Leemans *et al.*, Phys. Rev. Lett. **67**, 1434 (1991).
[16] J. F. Drake *et al.*, Phys. Fluids **17**, 778 (1974).
[17] W. P. Leemans *et al.* (to be published).
[18] R. W. P. McWhirter, in *Plasma Diagnostic Techniques*, edited by R. H. Huddlestone and S. L. Leonard (Academic, New York, 1965).
[19] J. M. Wallace *et al.*, Phys. Fluids B **3**, 2337 (1991).
[20] K. Estabrook, Phys. Rev. Lett. **41**, 1808 (1978).

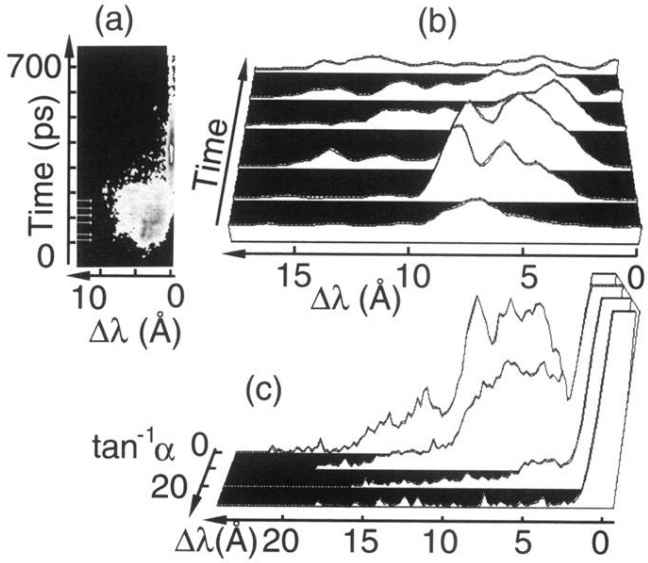

FIG. 1. (a) Streak-camera image of the Thomson-scattered probe beam in a H_2 plasma ($P=1.1$ Torr). Although not shown here, there was no blueshifted spectral feature visible in the original data. The white bar at the top indicates the location of a 100× attenuator for SBS. The peak intensity is 1.5×10^{14} W/cm^2. (b) Line outs of streak data taken along the direction of the arrows in (a). (c) Time-integrated streak-camera images of the Thomson-scattered probe beam in H_2 plasmas ($P=1$ Torr) for different degrees of ellipticity α of the laser polarization ($\tan^{-1}\alpha=45$ for circular polarization).